Nuclear Instruments and Methods in Physics Research A329 (1993) 291–298
North-Holland

NUCLEAR
INSTRUMENTS
& METHODS
IN PHYSICS
RESEARCH
Section A

^{222}Rn emanation into vacuum

Manqing Liu, H.W. Lee and A.B. McDonald
Department of Physics, Queen's University, Kingston, Ontario, Canada K7L 3N6

Received 3 November 1992

A low-background ZnS scintillator cell based on a design by Lucas has been developed for ^{222}Rn detection. Typical cells have 63% detection efficiency and 3 counts per day background. The cells have been used in measurements of ^{222}Rn emanation rate into vacuum from materials to be used under water in the Sudbury Neutrino Observatory (SNO) solar neutrino detector. The results are presented and the impact on the SNO detector design is discussed.

1. Introduction

ZnS-lined scintillator cells (Lucas cells) have been used in radon detection for over 30 years [1,2]. Most of the development work during this time has been concentrated on increasing detection efficiency. On the other hand, all these cells have relatively high background (0.05–0.3 cpm). A low background, reasonably high detection efficiency radon detector is required to determine the background caused by radon and its progeny in the Sudbury Neutrino Observatory (SNO), a heavy-water (D_2O) neutrino detector under construction near Sudbury, Ontario, Canada [3]. Fig. 1 shows the main parts of the detector. Neutrinos with sufficient energy interact in the D_2O to produce relativistic electrons or free neutrons. The neutrons are thermalized in the D_2O and are subsequently captured, generating γ-rays which in turn produce relativistic electrons. The electrons from either source will produce Cherenkov photons which pass through the D_2O, through the acrylic vessel which contains the D_2O, through the ultrapure H_2O used as background shielding and to the photomultipliers (PMTs) where they are detected.

The most serious source of background in the SNO detector (at a depth of 2030 m) is the radiation from naturally occurring radionuclides. ^{238}U and ^{232}Th and their daughters (particularly ^{214}Bi and ^{208}Tl) can contribute to the background by high-energy β- and γ-rays emitted in their decay. Monte Carlo calculations [3] shows that the tolerable concentration of the U chain in secular equilibrium is about 15×10^{-14} gU/g in the H_2O nearest to the acrylic vessel, and 1×10^{-14} gU/g in the D_2O.

The emanation of ^{222}Rn and ^{220}Rn and the leaching of their parent radium (^{226}Ra, ^{224}Ra) from materials into water can cause substantial disequilibrium in the water. The leaching of radium in the SNO detector is being studied by SNO collaborators at Oxford and Queen's [4]. There exists a body of literature on radon emanation from building materials (such as bricks, gypsum board, etc.) which have relatively high radium concentration. Measuring the ^{222}Rn emanation rate from low radioactivity detector materials such as stainless steel, signal cables and PMTs is the objective of the work reported in this paper.

By detecting ^{222}Rn, the rate of 2.45 MeV background gamma rays in the SNO detector from ^{214}Bi decay is determined directly even if there is disequilibrium in the radium or preceding long-lived nuclei. ^{222}Rn has a half-life of 3.8 day, but all daughters before ^{214}Bi have fast half-lives as shown in fig. 2. For each ^{222}Rn decay there are three alphas (^{222}Rn, ^{218}Po and ^{214}Pb). ^{220}Rn, with a 55 s half-life, is more difficult to detect and requires different techniques [4,5].

In the first section of this paper, the development of low background scintillation cells is described together with test results. Such cells were used in the measurements of ^{222}Rn emanation into vacuum discussed in the second section. These measurements were also carried out in such a way as to distinguish between ^{222}Rn outgassing and ^{226}Ra-supported radon emanation, which is more important in the SNO detector. In the third section the impact of ^{222}Rn emanation in the SNO detector and some further developments on the scintillation cell is discussed.

2. Development of a low-background scintillation cell

A Lucas cell detector consists of a chamber which is coated on the inside with silver-activated ZnS(Ag) scin-

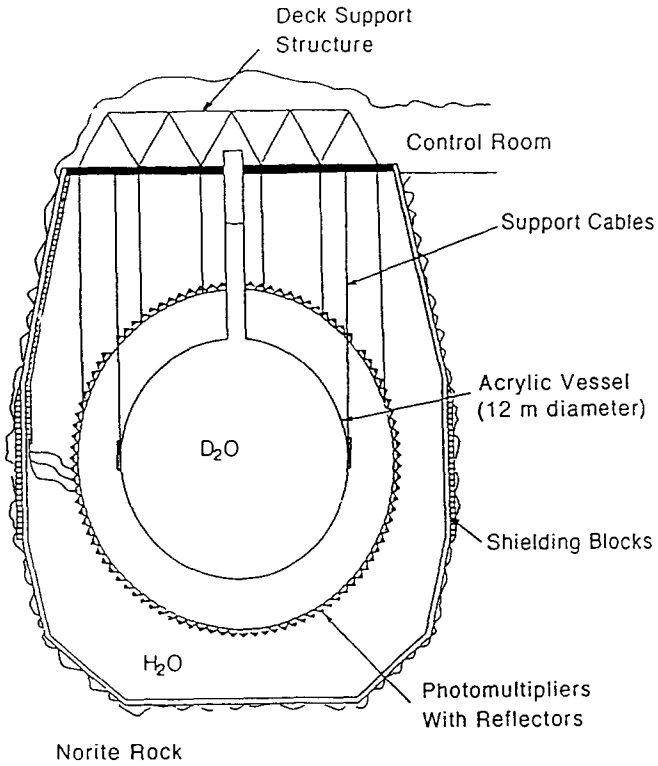

Fig. 1. Outline of the proposed SNO detector. The detector would be located at a depth of 2030 m (6800 feet) in INCO's Creighton mine near Sudbury, Ont. Canada.

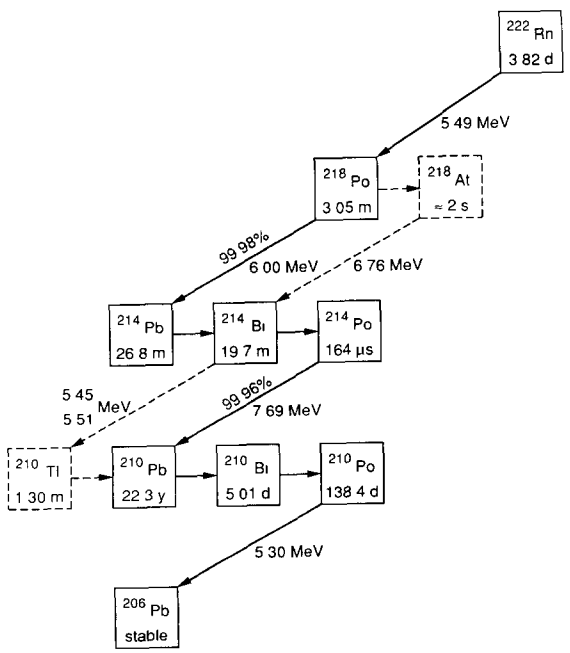

Fig. 2. Decay scheme of ^{222}Rn.

tillator. A photomultiplier is coupled to the window of the cell to detect the light emitted when an alpha particle from the decay of radon or its daughters strikes the ZnS. The cell is filled and sealed through a valve. Typically a Swagelok™ Quick-Connect is used because of its automatic shutoff feature when it is disconnected from the filling apparatus.

In order to have high detection efficiency, a large volume cell is often used [6]. However a larger volume needs more ZnS to coat the surface which results in a higher background. The largest volume with minimum surface area is a spherical design. The main factors considered in a new scintillation cell design are described below:

2.1. Cell body material

The material to be used for the cell body must have a low alpha particle surface-emission rate. Ultraviolet-transmitting (UVT) acrylic is one of the best among low radioactivity materials (< 10 ppt, U, Th [4,7]) and is also transparent. Methylene chloride solvent is used to seal an acrylic window to the cell body and to dissolve the acrylic surface to hold the ZnS coating.

2.2. ZnS sample selection

Six different ZnS (silver-activated) scintillator samples were tested for their relative light output and background. About 10 mg/cm^2 of ZnS was sandwiched between two flat pieces of acrylic sheet, taking care to seal the edges and exclude air. After a three day wait to allow ^{222}Rn and its daughters from residual air to decay, a PMT was coupled to one side and the background count rate was determined. The relative light output was determined by comparison of the pulse amplitude spectrum from each sample.

There was about a factor of 10 variation in the background rate and a factor of 5 variation in light output among the six samples tested. The sample from Johnson Associates (Montville, NJ, USA 07045) was selected as the best compromise between light output and background rate.

2.3. ZnS thickness optimization

The ZnS thickness has to be optimized for light yield and radioactivity background. The ZnS was coated onto a flat piece of acrylic by the following deposition method [8]. First the acrylic piece was submersed in a solution of ZnS suspended in ethyl alcohol. The ZnS slowly precipitated from the solution producing a uniform layer on the acrylic. The thickness of the ZnS layer was controlled by varying the deposition time. After the acrylic piece was taken out from the solution and dried, methylene chloride was used to fix the ZnS

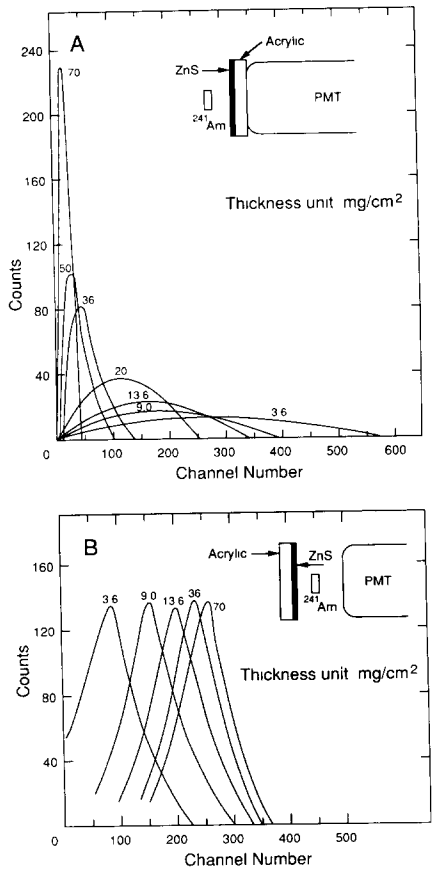

Fig. 3. Pulse height spectra for different ZnS thicknesses under (a) "transmission" geometry and (b) "reflection" geometry. The number above each curve is the ZnS thickness in mg/cm^2.

onto the acrylic. The ZnS thickness was determined from the difference in weight before and after the depositions

Two different geometries were investigated: "transmission" and "reflection". The pulse height spectra obtained using a ^{241}Am alpha source are shown in fig. 3 for these two cases. "Reflection" geometry (fig. 3b) gives an optimum ZnS thickness of about 10 mg/cm^2, equal to the range of a 5 MeV alpha particle in ZnS. Such a thickness of ZnS gives a reasonably high pulse amplitude compared to the PMT noise, and acceptable background contribution from the ZnS. This thickness was chosen for our cells.

2.4. PMT selection

A low noise PMT is preferred for low background measurements. However the light amplitude from the ZnS scintillator is much higher than the PMT noise amplitude, so the choice of PMT is not critical. Also the scintillation light from ZnS(Ag) peaks in the blue

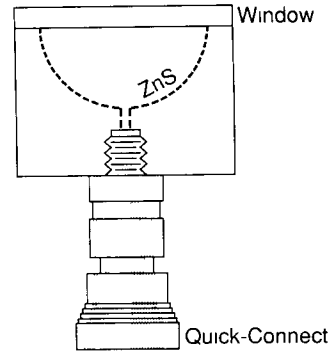

Fig. 4. Diagram of a 2 in. diameter hemispherical ZnS scintillation cell.

(4500 Å) region which matches the response of bialkali PMT photocathodes [9].

2.5. Cell shape

The shape of the Lucas cell was chosen to maximize the light striking the PMT and minimize the background. A hemispherical cell with a transparent window was designed. The outside diameter of the cell is two inches to match the diameter of the Philips XP2262B PMT chosen. Coating the cell window with a very thin ZnS layer results in higher detection efficiency but some of the pulses are degraded into PMT noise. We chose not to coat the cell window, thus sacrificing detector efficiency, but obtaining pulses clearly separated from the PMT noise.

The hemispherical two-inch diameter scintillation cell designed with the above considerations is shown in fig. 4. Fig. 5 shows a typical pulse height spectrum with the cell filled with radon. For comparison, fig. 5 also shows a spectrum obtained from a commercial Lucas cell [10] with a cylindrical shape. For the hemispherical design, the signals are very clearly separated from the

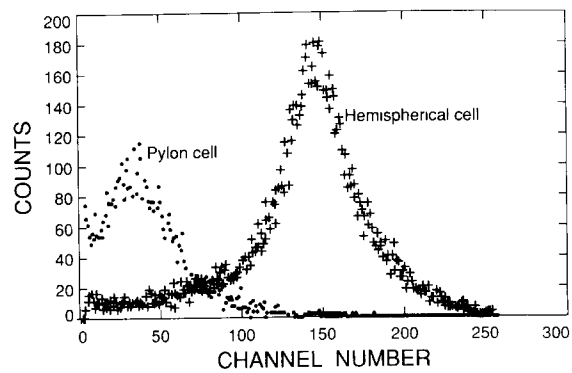

Fig. 5. Pulse height spectrum measured for the hemispherical cell illustrated in fig. 4. The spectrum measured with a commercial cell [10] is also shown in the figure.

PMT noise. Furthermore, the cell background was measured to be 3 counts per day for the new hemispherical cell (surface area = 20 cm^2), as compared to 3000 counts per day for the commercial cell (surface area = 145 cm^2). For the commercial cell, the type and thickness of ZnS, the method of ZnS deposition and the radioactivity of the cell body material (in this case aluminum) together give rise to the higher background.

We can rule out several sources which might produce background scintillations in the cell. Cosmic rays do not produce significant scintillation in the thin ZnS as determined by measurements with cosmic ray detectors in coincidence [11]. Beta and γ-rays from natural radioactivity also do not produce observable pulses. Assuming the air has a ^{222}Rn concentration of 2 pCi per liter [12], then our cell with a volume of 12 cm^3 and a typical residual pressure of less than 200 μm would have at most 6×10^{-2} counts per day. Acrylic even at a 100 ppt U level would give less than 1 count per day for our cell design. Hence the background of the cell is mainly from natural radioactivity in the ZnS. The alpha counting rate was measured to be about 15 counts per day per gram of ZnS. If we assume all these counts are from the ^{238}U decay chain alphas and the chain is in secular equilibrium, then the inferred U level is about 2×10^{-9} gU/g ZnS (i.e. 2 ppb).

The radon detection efficiency calibration for the hemispherical cells was done by putting a well determined amount of Rn into the cell and counting. The alpha counting rate was used to calculate the radon decay rate. The amount of Rn inside the cell was calibrated by Bigu [16]. The radon detection efficiency is defined as the ratio of the measured radon decay rate to the calculated radon decay rate, which was found to be $62 \pm 3\%$ compared to 66.6% of the geometric area covered with ZnS.

Additional background identification was done by recording the time associated with each event. For ^{222}Rn, the alpha from its decay is followed by the ^{218}Po ($t_{\frac{1}{2}} = 31$ min) alpha. The alpha from the decay of ^{220}Rn is followed by the ^{216}Po ($t_{\frac{1}{2}} = 0.14$ s) alpha. For total rates which are low (as in measuring the scintillation cell backgrounds), two events within 0.5 s of each other have a very high probability of being from ^{220}Rn. It is interesting to note that for an accumulated background run of 72 h on 30 mg of ZnS, we did not observe any ^{220}Rn decays, which indicates there is the equivalent of less than 5 ppb ^{232}Th in the ZnS.

3. ^{222}Rn emanation measurements

In materials, ^{226}Ra can occur in the grains, crystals, etc. making up the materials. When ^{226}Ra decays, some of the ^{222}Rn generated close to the surface of the grains can escape into the space between the grains by

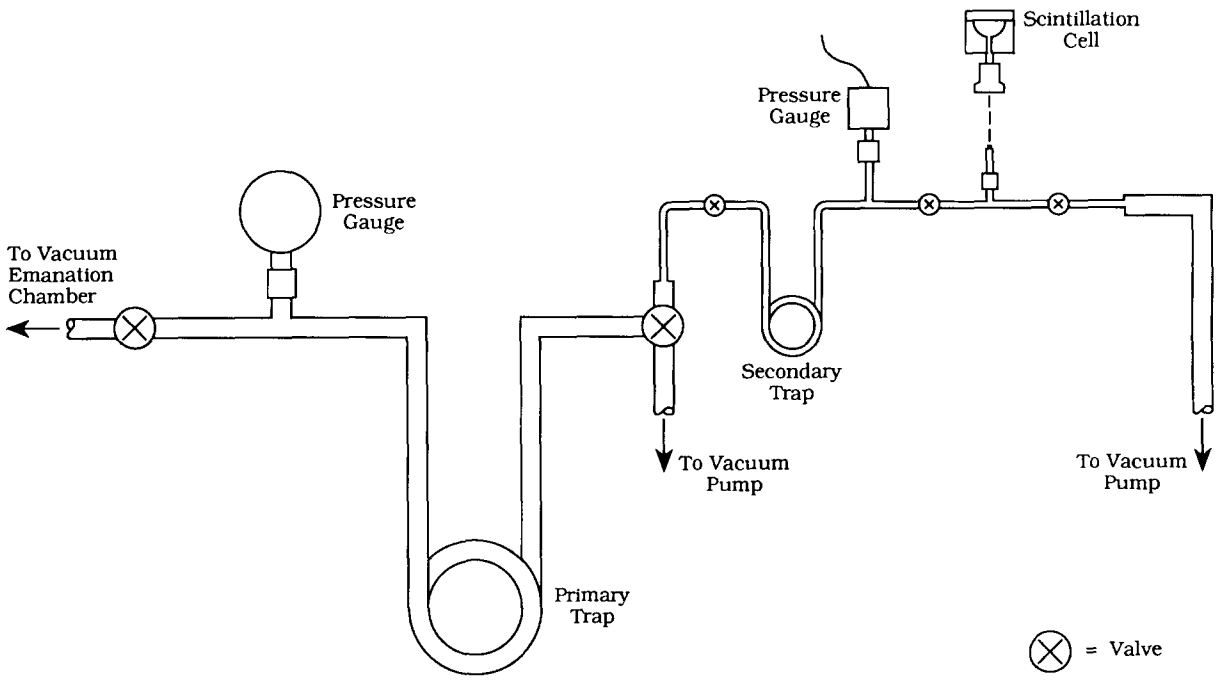

Fig. 6. Diagram of the radon emanation measurement system. The Rn was first trapped in the liquid-nitrogen cooled primary trap. Then the primary trap is warmed and the radon was transferred to the secondary trap immersed in liquid nitrogen. Finally the secondary trap was warmed and the radon was filled into the scintillation cell by free expansion.

virtue of their recoil energy. ^{222}Rn trapped deeper inside the grains and crystals can escape by diffusing out (outgassing). Only a fraction of the ^{222}Rn created by the decay of radium is given off to the outside; the remainder of the radon undergoes decay in the material. We describe a system and a procedure used to measure the rate at which ^{222}Rn is emanated by a material into vacuum.

The radon emanation system consists of the ^{222}Rn emanation chamber, ^{222}Rn transfer apparatus ("radon board") and hemispherical scintillation cell as shown in fig. 6. The radon emanation chamber is a cylindrical acrylic chamber with a 30 cm outer diameter and 65 cm long. Its wall thickness is 12 mm, and the ends are sealed with Viton O-rings. The purpose of the radon board is to extract radon from a mixture of trace gases (O_2, N_2) with lower freezing points and then transfer it into a scintillation cell. Its design is based on the one used by Key et al. [13] in studies of radium distribution in oceans. All the parts of the radon board are made of stainless steel Swagelok™ fittings. Brass wool was put into the traps to increase the ^{222}Rn trapping efficiency.

The radon collection efficiency of the system was calibrated by putting ^{222}Rn from a calibrated source into the emanation chamber, extracting the ^{222}Rn using the "radon board" and then putting it into the scintillation cell. The total efficiency is defined as the ratio of the radon decay rate of the scintillation cell after the extraction to the amount of ^{222}Rn put into the emanation chamber. A $33 \pm 4\%$ total efficiency was obtained, which includes $72 \pm 5\%$ efficiency for pumping the radon out of the emanation chamber into the liquid-nitrogen cooled primary trap, a $75 \pm 5\%$ efficiency for transferring the radon from the primary trap to the secondary trap and then into the scintillation cell and $62 \pm 3\%$ efficiency for detecting an alpha particle in the cell.

The background of the system was measured with no material placed inside the acrylic emanation chamber. Contributions to the background come from the acrylic chamber, the radon board and the scintillation cell. The lowest background achieved for the whole system was measured to be about 20 counts per day (where 12 counts per day were from the chamber, 5 from the radon board and 3 from the scintillation cell). It was found that the background rate in the chamber was higher shortly after large amounts of radon were emanated into the chamber by radioactive samples. The higher rate decreased with time at a rate consistent with the hypothesis that it comes from adsorption

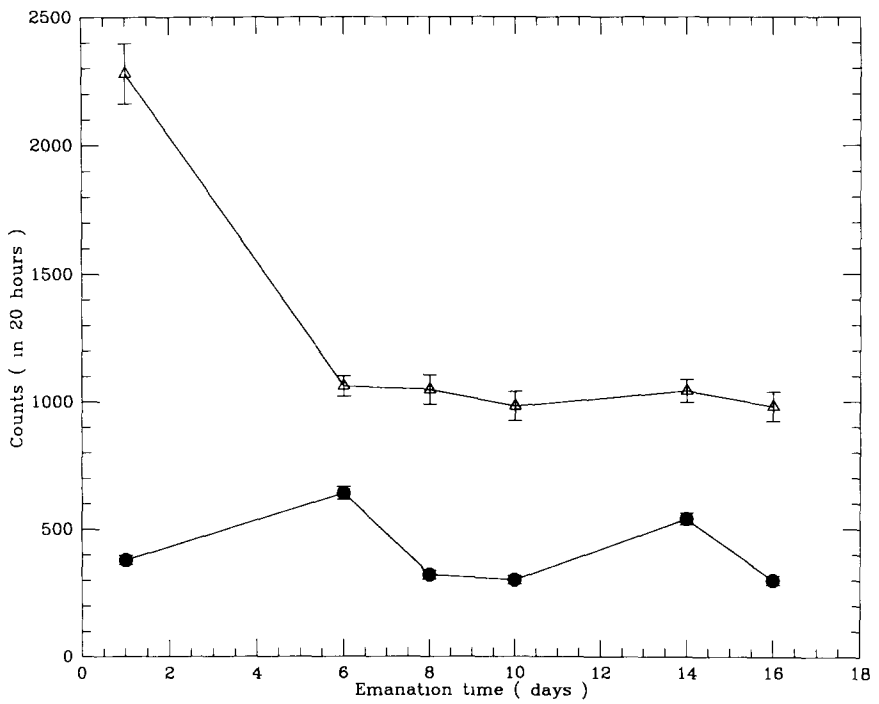

Fig. 7. Rn emanation measurement results from 9067 coax cable [●: before decay correction, △: after decay correction, $N_t/(1-e^{-\lambda t_i})$]. The horizontal axis represents the day which the chamber was opened, radon was extracted from the emanation chamber and resealed. It can be seen that the corrected emanation rates are nearly constant after a couple of days, indicating that the Rn is supported by Ra decay.

Table 1
Experimental Rn emanation rates into vacuum

Materials	^{222}Rn emanation rate	^{238}U content [7] [10^{-9} g/g (ppb)]
molecular sieve 13X	1200 ± 120 l^{-1}hr^{-1}	225 ± 19
activated charcoal	250 ± 50 l^{-1}hr^{-1}	
silica gel	440 ± 50 l^{-1}hr^{-1}	197
coax cable RG-59	60 ± 30 m^{-1}hr^{-1}	
twinaxial PE cable	< 2 m^{-1}hr^{-1}	
coax cable 8240	6 ± 2 m^{-1}hr^{-1}	
coax cable 9067	< 0.6 m^{-1}hr^{-1}	< 10
Kevlar 3/8 in. rope	< 0.3 m^{-1}hr^{-1}	0.07
8 in. diameter PMT	< 20 PMT^{-1}hr^{-1}	
low-rad. glass	< 1.6 m^{-2}hr^{-1}	50
aluminum reflector	< 1.5 m^{-2}hr^{-1}	
black ABS plastic	< 1.1 m^{-2}hr^{-1}	20 ± 5
white polyethylene	< 0.9 m^{-2}hr^{-1}	
acrylic	< 0.1 m^{-2}hr^{-1}	
Al plates	< 0.5 m^{-2}hr^{-1}	5
SS 304L [supplier 1]	< 15 m^{-2}hr^{-1}	< 1
SS 304L [supplier 2]	< 0.3 m^{-2}hr^{-1}	

of ^{222}Rn on the walls of the chamber. The scintillation cell background increases by 1 count a day for every 10^4 ^{222}Rn decays in the cell because of the 22 year ^{210}Pb (fig. 2).

The measurements of radon emanation from materials were performed in the following way. The material for which the ^{222}Rn emanation was to be measured was put inside the emanation chamber and pumped for more than a day. Typically the chamber reached a vacuum of 200–500 microns. Then the chamber was sealed in order for the ^{222}Rn to emanate. After a time t_1 the ^{222}Rn in the chamber was extracted (for 30 to 45 min) and transferred to a scintillation cell. After a 3 h wait for ^{222}Rn and daughters decays to come to equilibrium, the number of counts N_1 was obtained for 20 h of counting. The chamber was sealed after the ^{222}Rn extraction and the procedure was repeated for emanation times t_2, t_3, etc. over about 10 days total, each time using a new scintillation cell. By plotting $N_i/(1 - e^{-\lambda t_i})$ as a function of the cumulative time, it is possible to distinguish outgassing of absorbed radon from Ra-supported Rn emanation. For ^{226}Ra-supported ^{222}Rn emanation, the function would be a constant value. Contributions from outgassing of absorbed radon produce excess counts for times less than about 4 days. If radon emanation from ^{226}Ra decay was clearly observed, an average value for emanation times much greater than 4 days was determined, together with an uncertainty. In situations with low statistics or without an observable steady emanation rate, only an upper limit for Ra-supported ^{222}Rn emanation could be determined.

The experimental results are summarized in table 1. In most instances, only an upper limit for the ^{222}Rn emanation rate was obtained. As an example of the results, fig. 7 shows the time evolution of the emanated ^{222}Rn for coax cable 9067 (high-density polyethylene outer jacket). There is some outgassing of absorbed radon initially and after several days all the ^{222}Rn is supported by ^{226}Ra decay in the cable.

Table 2
Rn emanation in the SNO detector

Material	Quantity	^{222}Rn emanation rate	Supported ^{222}Rn
Between the PMT support structure and the acrylic vessel			
acrylic vessel	452 m^2	< 0.1 m^{-2}hr^{-1}	$< 6 \times 10^3$
suspension rope (Kevlar)	180 m	< 0.3 m^{-1}hr^{-1}	$< 7 \times 10^3$
PMT glass	473 m^2	< 1.6 m^{-2} hr^{-1}	$< 1 \times 10^5$
Al reflectors	673 m^2	< 1.5 m^{-2}hr^{-1}	$< 1 \times 10^5$
ABS in PMT support structure	3665 m^2	< 1.1 m^{-2}hr^{-1}	$< 5 \times 10^5$
stainless steel	410 m^2	< 0.3 m^{-2}hr^{-1}	$< 2 \times 10^4$
mine dust (0.4 μg/cm^2)	23 g	44 g^{-1}hr^{-1} [15]	1.3×10^5
Total			$< 9 \times 10^5$
Outside the PMT support structure			
stainless steel	650 m^2	< 0.3 m^{-2}hr^{-1}	$< 3 \times 10^4$
coax cables [a]	190000 m	< 0.6 m^{-1}hr^{-1}	$< 1 \times 10^7$
plastic liner	2000 m^2	2 m^{-2}hr^{-1} [b]	5.3×10^5
ABS in PMT support structure	1250 m^2	< 1.1 m^{-2}hr^{-1}	$< 2 \times 10^5$
dust (4 μg/cm^2) [b]	256 g	44 g^{-1}hr^{-1} [15]	1.5×10^6
Total			$< 1 \times 10^7$

[a] The coax cables will be bundled and the exposed area is estimated to be 2500 m^2.
[b] Design goal.

A ^{222}Rn emanation rate can be calculated by assuming that it recoils directly out from a ideal smooth surface because of its kinetic energy. This calculated ^{222}Rn emanation rate for known recoil ranges and bulk radioactivity is about 1000 times lower than the observed Ra-supported ^{222}Rn emanation rates. This suggests that ^{222}Rn is diffusing out from the decay of ^{226}Ra deeper within the material.

4. Impact on the SNO detector design

The ^{222}Rn emanation rates of the major components of the SNO detector have been measured. If the ^{222}Rn emanation rate into water is similar to that into vacuum, then the total ^{222}Rn emanated from submersed materials in the water can be calculated.

The H_2O (fig. 1) is divided into an "inner" volume (1700 ton) between the PMT support structure and the acrylic vessel and an "outer" volume (5500 ton) between the PMT support structure and the cavity liner. A 99% water-tight seal on the PMT support structure reduces mixing of H_2O in the outer region with the more critical low-radioactivity H_2O inside. There will not be a significant amount of emanated radon in the D_2O because there is very little material other than clean acrylic in contact with it. The ^{222}Rn emanated from the submersed materials in the two volumes of H_2O are presented in table 2. The last column ("Supported ^{222}Rn") is given by the product of the area or length, the emanation rate and the mean life of ^{222}Rn (3.8 day/ln 2).

During the assembly of the detector, some mine dust will be deposited on the surfaces, in spite of extreme care with cleanliness. The final cleanup is expected to reach a level of 0.4 μg dust per cm^2 inside the PMT support structure [4] which gives a total of 23 g of dust over the 5673 m^2. The dust outside the PMT support structure will be harder to clean up because the surfaces have many hidden crevices. There we are aiming for 4 μg of dust per cm^2 which over the 6400 m^2 gives 256 g of dust.

The total emanated radon in table 2 can be compared to the design objective for the SNO detector. The 1700 tonnes of H_2O inside the PMT support structure is expected to contain less than 15.0×10^{-14} gU/g (which supports 1.5×10^6 radon) and the 5300 ton of H_2O outside the PMT support structure should contain less than 45.0×10^{-14} gU/g (which supports at least 4.5×10^6 radon). As shown in table 2, the emanated radon load outside the PMT support structure could be higher than the emanated radon load inside the structure. The H_2O water recirculation system will take water from the outer region, put it through ion exchange resins, high efficiency vacuum degassing and ultraviolet radiation before returning it to the critical inner H_2O volume.

Two other sources of radon are the plastic cavity liner and the cover gas above the H_2O and D_2O surfaces. The design goal for the cavity liner is to have no more than 2 ^{222}Rn m^{-2}hr^{-1} penetrating through the liner into the water. Independent measurements indicate that the design goal can be met [16]. If the cover gas is constrained to contain less than 2×10^{-4} pCi/liter of radon, then the exchange of radon into the water will not be a significant problem [14].

5. Further development on scintillation cells

The transfer efficiency of radon to a scintillation cell can be improved by immersing the scintillation cell into liquid nitrogen while the Rn is being transferred. One effect of doing this is an effective increase of the pressure in the cell by a factor of 4 due to the lower temperature. The other effect is that the inner surface of the cell becomes a cryogenic pump for radon.

We have developed several cell designs which survive repeated submersion in liquid nitrogen. With this apparatus, nearly all of the Rn collected in the primary ^{222}Rn trap can be transferred into the cell. We are continuing to work on the reliability of the cell design as some have developed cracks in the window seal.

6. Conclusion

A low background, high efficiency scintillation cell has been developed for ^{222}Rn detection for the SNO detector. If the ^{222}Rn emanation rate into water is similar to that into vacuum, then the total Rn emanated into the SNO detector is less than the design objectives.

Acknowledgements

We are grateful to Dr. J. Bigu (CANMET, Elliot Lake, Canada) for his assistance in the efficiency calibration of the hemispherical scintillation cell. We wish to thank G. Mathieu at Lamont–Doherty Geological Observatory (Palisades, NY) for supplying samples of ZnS and Drs. P. Jagam and J. Simpson (University of Guelph) for measurements of U and Th content in materials. We also thank Drs. R. Key (Princeton University), R. Kouzes (Princeton University), D. Sinclair (Centre for Research in Particle Physics, Ottawa) and B. Sur (Queen's University) for many helpful discussions.

References

[1] H.F. Lucas, Rev. Sci. Instr. 28 (1957) 680.
[2] A.C. George, IEEE Trans. Nucl. Sci. NS-37 (1990) 892.
[3] G.T. Ewan et al., Sudbury Neutrino Observatory (SNO) Proposal, SNO-87-12 (1987);
SNO Scientific and Technical Description of Mark II detector, ed. E. Beier, D. Sinclair (SNO-89-15, 1989);
see also G.T. Ewan, Nucl. Instr. and Meth. A314 (1992) 373.
[4] C.E. Waltham, E.D. Hallman, P. Doe, R.G.H. Robertson, W. Frati, R. Van Berg, K.T. Lesko, B.C. Robertson and J.J. Simpson, Phys. in Can. 48 (1992) 135.
[5] B. Sur, H. Lee, X. Zhu, M.-Q. Liu and A.B. McDonald, Bull. Amer. Phys. Soc. 37 (1992) 1020.
[6] B.L. Cohen, M. Elgayni and B. Duchemin, Nucl. Instr. and Meth. A286 (1990) 594.
[7] P. Jagam, J.-X. Wang and J.J. Simpson, submitted to J. Radioanal. Nucl. Chem.;
E.D. Earle and E. Bonvin, Sudbury Neutrino Observatory Report, SNO-STR-92-061 (1992).
[8] Manqing Liu, M.Sc. thesis, Dept. of Physics, Queen's University, Kingston, Canada (1991).
[9] T. Hase, T. Kano, E. Nakazawa and H. Yamamoto, Adv. in Elect. and Electron Phys. 79 (1990) 271.
[10] Pylon Electronic Development Company Ltd., Ottawa, Ontario (Canada).
[11] R. Kouzes, Princeton University, private communication.
[12] W.W. Nazaroff and A.V. Nero (eds.), Radon and its Decay Products in Indoor Air (John Wiley, 1988).
[13] R.M. Key, R.L. Brewer, J.H. Stockwell, N.L. Guinasso and D.R. Schink, Mar. Chem. 7 (1979) 251.
[14] B. Sur, Sudbury Neutrino Observatory Report, SNO-STR-91-055 (1991).
[15] X. Zhu, Queen's University at Kingston, Canada, private communication.
[16] J. Bigu, CANMET, Elliot Lake, Canada, private communication.